Oceanologia, 67 (3)/2025, 67305
Polish Academy of Sciences
Institute of Oceanology

https://doi.org/10.5697/WXXI2926

Quantile mapping enhances the sea surface temperature prediction accuracy in the northern coastal region of Penang using ROMS

Ninu Krishnan Modon Valappil, Chin Alice, Abigail Birago Adomako, Ehsan Jolous Jamshidi, Yusri Yusup *

Abstract
Sea surface temperature (SST) is a crucial climate indicator for tracking atmospheric and oceanic interactions, particularly in coastal areas. The study focused on the simulation of SST in the region around the north coast of Penang Island, Malaysia, where the prediction of SST is challenging due to its complex atmospheric and oceanic interactions. The Regional Ocean Modeling System (ROMS), a sophisticated numerical model, is employed to predict the variation of SST in the study region. In the present study, HYCOM Global Ocean Forecasting System (GOFS) was incorporated to generate the boundary condition, initialisation, and climatology, while MERRA-2 datasets were considered as atmospheric forcing datasets. The generated SST from ROMS was compared with Aqua-MODIS observations of SST across six selected locations. Different methods, such as time series plots, linear modelling plots, and Taylor diagrams, and error estimation methods were employed to understand the accuracy of the model. The result indicates an underestimation of the SST using the ROMS model. Also, the root mean square error (RMSE) and mean absolute error (MAE) show an average of 2.58°C and 2.50°C in the study area, highlighting the requirement for bias correction. Three bias correction methods, such as Delta Change (DC), Linear Scaling (LS), and Quantile Mapping (QM), were considered to improve SST predictions. The comparative analysis of these three methods through time-series plots and statistical evaluations demonstrates that all three methods significantly reduce errors by bringing RMSE and MAE below 0.7°C. It is also noted that the best result was obtained by the QM method, as it not only reduces mean errors but also enhances correlation between the predicted and observed SST, the other two methods show no variation in the correlation value. The study confirms that the ROMS model can effectively capture the characteristics fluctuation of the SST in the dynamic regions like the north coast of Penang Island but bias correction is crucial for improving the prediction. In this case, the QM bias correction method provides the most balanced and effective adjustment compared to the other two methods.

Keywords
ROMS Model; SST; Statistics; RMSE; Error matrix

Environmental Technology Division, School of Industrial Technology, Universiti Sains Malaysia, 11800 USM, Penang, Malaysia
***Correspondence**: yusriy@usm.my (Y. Yusup)

Received: 25 June 2025; **revised:** 2 August 2025; **accepted**: 11 August 2025

1. Introduction

Sea surface temperature (SST) serves as an integral part in modulating the physical, chemical, and biological dynamics within marine ecosystems (Mann and Lazier, 2005). It has a significant impact on ocean-atmosphere interactions, which in turn affects meteorological phenomena, ocean currents, and the holistic framework of the global climate system. Fluctuations in SST can instigate alterations in wind dynamics, precipitation patterns, and the development of cyclonic systems, which subsequently affect coastal and marine ecological networks (Ottersen et al., 2004; Hewitt et al., 2016; Piccolo, 2021; Wang et al., 2024). For instance, elevated SST anomalies are frequently associated with severe meteorological occurrences such as tropical cyclones and marine heatwaves, both of which can trigger significant damage on marine habitats and coastal infrastructure (Hobday et al., 2016). This interaction is identified in phenomena like El Niño and La Niña, where fluctuation in equatorial Pacific Ocean SST can lead

to widespread climatic effects, including altered precipitation patterns and temperature anomalies across the globe (McPhaden et al., 2006). In addition to that, the fluctuation in SST can impact the transport of nutrients and carbon cycling by influencing the density of seawater, which is essential for driving the global conveyor belt of ocean currents. This will ultimately damage the biological productivity and marine ecosystem (Williams and Follows, 2003; Whitney et al., 2005; Satar et al., 2024; Guan et al., 2025; Guild et al., 2025). In light of these widespread implications, the ongoing surveillance and precise modelling of SST is imperative for the comprehension and forecasting of transformations within both regional and global climatic contexts.

Even though the introduction of satellite based measurements provide extensive and continuous monitoring of ocean temperature across wide areas including those regions that are difficult to carry out in situ measurements, these measurements can cover only the surface temperature of Ocean (Barton, 1995; Casey and Cornillon, 1999; Merchant et al., 2019; Huang et al., 2021; Embury et al., 2024). The presence of a mixed layer nature makes disparity in the measurements because of the complicated and fluctuating vertical temperature structure of the upper ocean due to ocean turbulence, air-sea fluxes of heat, moisture, and momentum.In addition to that, the availability of the continuous measurements of satellite-based SST can vary based on disruptions due to technical failures, sensor degradation, or changes in climate conditions (Dubovik et al., 2021; Li et al., 2023; Embury et al., 2024; Shevchenko et al., 2024). So, another source of SST data with better quality and continuous measurement is needed for both operational forecasting and scientific research. The ocean circulation model is an alternative or complementary approach to understand the SST because of its long term prediction capability and potentially high accuracy. To simulate SST, various models have been developed with different methodologies, capabilities, and advantages that range from a simple statistical approach to advanced ocean-atmospheric models (O'Carroll et al., 2019; Haghbin et al., 2021; Alizadeh, 2022; Vanem et al., 2022; Kartal, 2023; Zrira et al., 2024). The detailed insight into the ocean dynamics can be understood by numerical ocean circulation models like ROMS and HYCOM, while for long-term climate prediction a coupled climate models such as CESM and CMIP are essential. The short term prediction of SST can be efficiently obtained by statistical models, whereas machine learning based approaches bring new capabilities in data-driven ocean forecasting.

The Regional Ocean Modeling System (ROMS) is a free surface and terrain-following data assimilative ocean circulation model. It is a four-dimensional modelling system which is widely used to simulate oceanic circulation patterns that follow the Earth System Modelling Framework (ESMF) conventions for model coupling. The accuracy and performance of the ROMS model vary across different regions and time periods. A number of studies were documented to understand the performance and accuracy of the model, specifically SST, for the prediction and forecasting. In the Gulf of Thailand and neighbouring area Kaewmesri (2019) conducted a study to simulate SST using ROMS model. They considered the Generic Length Scale (GLS) vertical mixing method to simulate SST over 31 May, 30 June, and 31 July, 2018, with a horizontal resolution and vertical levels of 10 km × 10 km and 40 layers, respectively. They noted that the ROMS model SST pattern shows a good agreement with NOAA Optimum Interpolation Sea Surface Temperature (OISST) observational data. Kushwaha et al. (2024) conducted a study to simulate the SST variability across the Arabian Sea during the period from 1992 to 2021 by considering the ROMS, version 3.7 and a horizontal resolution of 1/4°. According to them, the comparison of the simulated result shows a reasonable agreement with the observational and reanalysis data. They also noted that the seasonal variation was captured by the model very efficiently.

Tiwari et al. (2021) conducted a study to simulate the SST in the Indian Ocean using the ROMS model by considering different atmospheric forcing, such as the National Centers for Environmental Prediction (NCEP), National Centre for Medium-Range Weather Forecasting (NCMRWF), and TropFlux. They noted that TropFlux and NCMRWF give almost similar results in comparison with the observational data, but NECP was unable to capture the variability of SST, especially over the central part of the Arabian Sea. Costa et al. (2012) developed an Ocean modelling system with a horizontal resolution of 1/36° based on the ROMS model for the northwestern Iberian Peninsula by considering the MERCATOR ocean system for the North Atlantic (horizontal resolution 1/6°) and forcing the Weather Research and Forecasting Model (WRF) and the Soil Water Assessment Tool (SWAT). They noted that over a period of one year absolute error of the SST is less than 1°C during the validation with the real-time SST observational network from the Meteo Galicia, INTECMAR, and Puertos Del Estado. Water temperature in the Bohai Sea, the Yellow Sea, and the East China Sea was simulated with high resolution by Han and Wang (2022) based on the ROMS model. They noted seawater temperature simulated by the ROMS model shows a close result when compared with the WOA13 data and previous research data. Given the use of ROMS for modelling and forecasting SST in different regions, this study aims to assess its effectiveness and suitability for analysing spatial and temporal SST variations off the northern coast of Penang Island, Malaysia. The selected region experiences a range of atmospheric and oceanic circulations that influence the physical and chemical properties of the seawater. Additional information regarding the study area and the datasets utilized will be provided in the subsequent section.

2. Study area

The current research focuses on the northern coast of Penang Island, situated in the Malacca Strait. A grid was established, encompassing north latitudes, from 3°20′31.0′′N to 6°05′36.0′′N, and east longitudes, from 98°38′01.0′′E to 100°19′08.0′′E, as illustrated in Table 1. For the comparative analysis of SST, six specific locations along the northern coast of Penang Island were selected, as depicted in Figure 1. Detailed information regarding these six sites, including target, ROMS, and Aqua MODIS data, is provided in Table 2. The area is characterized by a tropical climate, marked by consistently high temperatures and humidity levels throughout the year. Additionally, the region is affected by the Malaysia Current, a warm and shallow current that flows northward along the western coast of Peninsular Malaysia from the South China Sea, significantly influencing salinity, water temperature, and nutrient distribution.

Table 1. Coordinates of the grid selected for the present research.

Selected coordinates	Latitude and longitude
C1	4°44′19.0′′N, 97°51′33.0′′E
C2	6°05′36.0′′N, 100°19′08.0′′E
C3	4°41′58.0′′N, 101°05′37.0′′E
C4	3°20′31.0′′N, 98°38′01.0′′E

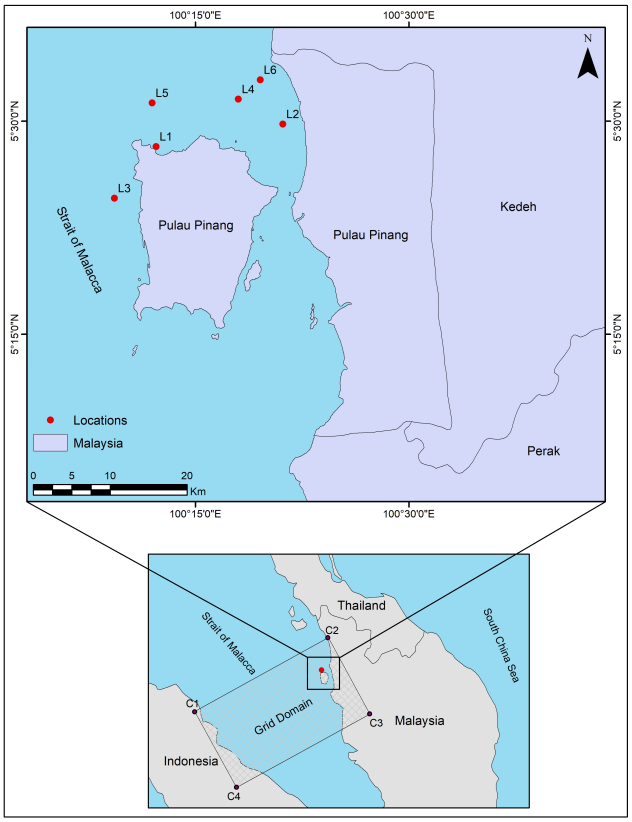

Figure 1. Study area map with selected locations to compare the ROMS SST with Aqua MODIS SST.

3. Datasets and methodology

3.1 ROMS model generation

Before initializing the ROMS model, a grid domain consisting of 150 × 300 cells was generated using GridBuilder. This grid domain was subsequently exported in NetCDF format for use as model input. A more accurate land-sea mask was created by refining the masking process with GSHHG Coastlines. Additionally, bathymetry was smoothed through the application of a Shapiro Filter and Positive Adjustment to mitigate inaccuracies in pressure gradients that could potentially destabilize the model simulation. Furthermore, data sourced from the HYCOM Global Ocean Forecasting System (GOFS) 3.1, developed by the Navy Coupled Ocean Data Assimilation (NCODA) at the Naval Research Laboratory, were utilized to produce the initialization, climatology, and boundary condition input files. These HYCOM datasets were remapped to the specific study area prior to being incorporated into the ROMS model. The initialization file generated from GOFS 3.1, which includes a 41-layer HYCOM and NCODA Global 1/12° Analysis, contains essential variables such as free-surface, two-dimensional momenta, and tracers including temperature, salinity, sea surface height (SSH), and u-v currents. These variables were downloaded and extracted from the OpenDAP server via the THREDDS catalogue platform using Python scripts and the PyROMS package. For this research, a single initialization file was sufficient, particularly for the initial day of the study period, whereas a climatology file encompassing the full duration of the study (from November 1, 2019, to December 31, 2019) was essential.

The atmospheric forcing data utilized in this research is derived from the Modern-Era Retrospective Analysis for Research and Applications, Version 2 (MERRA-2). The specific MERRA-2 datasets employed in this analysis include M2T1NXRAD, M2T1NXSLV, and M2T1NXINT. Key variables such as total precipitation, air pressure (P_{air}), air humidity (Q_{air}), air temperature (T_{air}), wind speed in the u-v direction (U_{wind} and V_{wind}), albedo, cloud cover, surface incoming shortwave radiation (SWRAD), and surface absorbed longwave radiation (LWRAD) were extracted and imported into ROMS. Following the initial setup, the configuration of the roms_upwelling.in file was completed, detailing grid spatial dimensions, lateral boundary conditions, time- stepping protocols, various physical coefficients and constants, vertical coordinate systems, and logical switches and flags to manage output frequency, as well as the names of input and output NETCDF files for data import and export, along with other scripts for data assimilation. Subsequently, the model was executed on a Linux platform, and the SST data for the study period were extracted from the ROMS output for subsequent analysis.

Table 2. Locations selected for the comparative analysis of SST from ROMS and Aqua MODIS.

Location	Coordinate points (latitude, longitude)		
	Target location	ROMS	Aqua-MODIS
L1	5°28′12.8″N, 100°12′14.5″E	5°28′09.7″N, 100°12′47.6″E	5°28′45.0″N, 100°11′15.0″E
L2	5°29′47.8″N, 100°21′08.5″E	5°29′44.6″N, 100°20′58.2″E	5°28′45.0″N, 100°21′15.0″E
L3	5°24′34.5″N, 100°09′18.8″E	5°24′34.8″N, 100°09′36.4″E	5°23′45.0″N, 100°08′45.0″E
L4	5°31′33.7″N, 100°18′01.4″E	5°31′26.9″N, 100°17′26.1″E	5°31′15.0″N, 100°18′45.0″E
L5	5°31′17.4″N, 100°11′57.9″E	5°31′30.1″N, 100°12′13.8″E	5°31′15.0″N 100°11′15.0″E
L6	5°32′54.9″N, 100°19′34.1″E	5°32′49.1″N, 100°19′15.7″E	5°33′45.0″N, 100°18′45.0″E

3.2 Aqua-MODIS satellite data

In the present research aimed at validating the SST derived from the ROMS, SST data were obtained from the Moderate Resolution Imaging Spectroradiometer (MODIS) onboard the Aqua satellite, which was launched in 2002. The Level 3 Daily SST data, characterized by a spatial resolution of 4 km, were retrieved from NASA's Ocean Color Web for the period spanning from November 1, 2019, to December 31, 2019. In addition to Level 3 datasets, NASA's Ocean Color Web provides access to other processing levels, including Level 2 in swath format with a higher resolution of 1 km, and Level 4, which offers gap-free, cloud- free global data (Kilpatrick et al., 2001). Furthermore, various temporal resolutions, such as daily, weekly, and monthly datasets, are also available.

3.3 Comparison of the modelled data

To compare the analysis results, a range of techniques were employed, such as time series plots, linear modeling plots, Taylor diagrams, and error evaluation using Root Mean Square Error (RMSE) and Mean Absolute Error (MAE). These methods were used to demonstrate the accuracy of the ROMS modelled data in comparison to the data measured by satellites.

3.4 Error Estimation methods

To evaluate the precision and effectiveness of the ROMS-modeled SST, the RMSE and MAE were utilized. The RMSE can be calculated as (Mendez et al., 2020; Jose and Dwarakish, 2022).

$$\mathrm{RMSE} = \sqrt{\frac{\sum \left(\mathrm{SST}_{\mathrm{Aqua}} - \mathrm{SST}_{\mathrm{ROMS}}\right)^2}{n}} \tag{1}$$

and MAE can be calculated as

$$\mathrm{MAE} = \frac{\sum \left|\mathrm{SST}_{\mathrm{Aqua}} - \mathrm{SST}_{\mathrm{ROMS}}\right|}{n} \tag{2}$$

where n is the length of the datasets.

3.5 Bias correction methods

Various bias correction techniques were utilized to adjust the modeled SST data from the ROMS model, including the Delta Change (DC) method, Linear Scaling (LS) method, and Quantile Mapping (QM) method. A detailed explanation of each method is provided below.

3.6 Delta Change (DC) method

The Delta Change (DC) method represents the most straightforward approach for addressing systematic errors. This model operates under the premise that regional biases remain stable over time. In this approach, the corrected SST from the ROMS is derived by incorporating the difference (delta) between the average SST produced by the ROMS and the average SST obtained from Aqua MODIS at each time interval. Consequently, the DC-corrected ROMS SST can be expressed as outlined by Lemos et al. (2020) and Beyer et al. (2020).

$$\mathrm{SST}^{\mathrm{DC}}_{\mathrm{ROMS}}(t) = \mathrm{SST}_{\mathrm{ROMS}}(t) + \Delta \tag{3}$$

where

$$\Delta = \overline{\mathrm{SST}_{\mathrm{Aqua}}} - \overline{\mathrm{SST}_{\mathrm{ROMS}}} \tag{4}$$

3.7 Linear Scaling (LS) method

The linear scaling (LS) method is a regression-based correction technique that is utilized when there is a linear correlation between the bias and the observed SST (Acharya et al., 2013). This approach involves modifying the model output through a linear transformation derived from the observed data. The SST from the ROMS that has been corrected using the LS method can be expressed as

$$\mathrm{SST}^{\mathrm{LS}}_{\mathrm{ROMS}}(t) = a \times \mathrm{SST}_{\mathrm{ROMS}}(t) + b \tag{5}$$

where a is the scaling parameter and b is the offset parameter.

3.8 Quantile Mapping (QM) method

The Quantile Mapping (QM) technique is a non-linear approach that employs a transfer function to perform bias correction (Ringard et al., 2017). This method involves adjusting the distribution function of the modeled data to align with the distribution of the observed data. It effectively addresses bias in the distribution shape, as noted by Dhawan et al. (2024). The formula utilized for implementing the QM bias correction is

$$\mathrm{SST}_{\mathrm{ROMS}}^{\mathrm{QM}} = F_{\mathrm{Aqua}}^{-1}(F_{\mathrm{ROMS}}(\mathrm{SST}_{\mathrm{ROMS}})) \tag{6}$$

where F_{ROMS} is the cumulative distribution function of the ROMS data, and F_{Aqua}^{-1} is the inverse cumulative distribution of the Aqua MODIS data.

In quantile mapping, the cumulative distribution function (CDF) is derived directly from observed data through a non-parametric method. To create the CDF, datasets – such as ROMS sea surface temperature (SST) and Aqua MODIS SST – are initially arranged in ascending order. Each value in this ordered list is subsequently assigned a cumulative probability (quantile) according to its rank. A frequently utilized formula for calculating this probability is $F(x_i) = i/n + 1$, where i represents the rank (position) of the value within the sorted dataset, and n denotes the total number of data points (Cunnane, 1989). This process results in a uniformly distributed set of cumulative probabilities that correspond to the sorted ROMS SST values, collectively forming the CDF of the ROMS model output. Given that this CDF is discrete and confined to the available data points, it may not yield precise matches for all input values – particularly those that lie between observed points. To remedy this, linear interpolation is employed to estimate cumulative probabilities (quantiles) or related SST values for intermediate inputs. This interpolation guarantees a smooth and continuous mapping, which is crucial for the quantile-to-quantile correction process inherent in quantile mapping.

4. Results and discussion

In this study, various techniques were employed, including time series analysis, linear modelling, Taylor diagrams, and the calculation of error metrics such as RMSE and MAE, to assess the accuracy of SST modelled by the ROMS in relation to SST data obtained from Aqua-MODIS. The findings from each analysis are elaborated upon in the sections that follow.

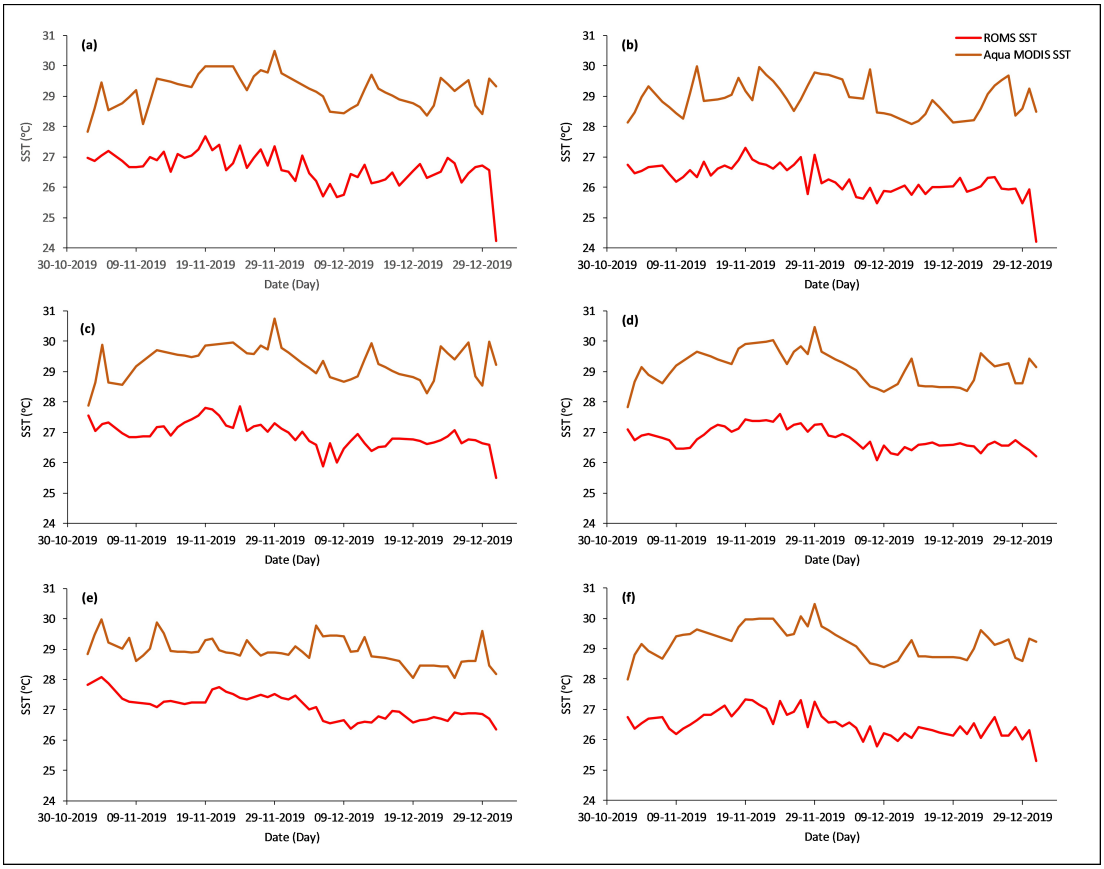

Figure 2. Time series plot comparing the SST data from ROMS and Aqua-MODIS for the period of November to December 2019 at the specified locations: (a) L1, (b) L2, (c) L3, (d) L4, (e) L5, and (f) L6.

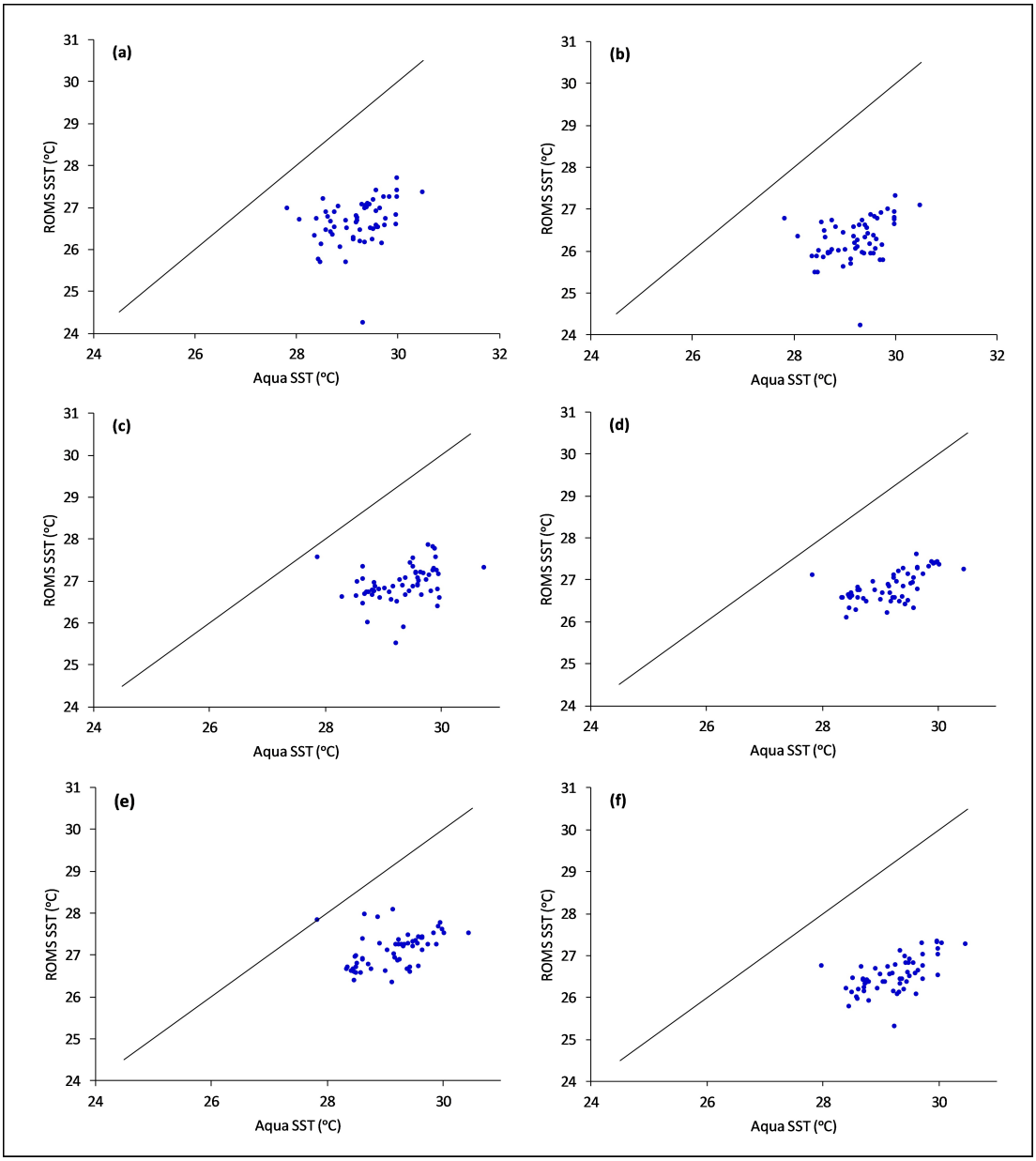

Figure 3. Linear modelling plots that illustrate the comparison between ROMS SST and Aqua-MODIS SST at the following locations: (a) L1, (b) L2, (c) L3, (d) L4, (e) L5, and (f) L6.

4.1 Time-series plot

In this study, six time-series graphs representing daily sea surface temperature (SST) from both the ROMS and Aqua MODIS were generated for six unique locations, as shown in Figure 2 (a to f). The MODIS dataset used covers the period from November 1, 2019, to December 31, 2019, and there are particular occurrences of missing values within the MODIS data. These data gaps were filled using nearest neighbour and average filling methods, and utilized in further analysis. The analysis reveals that during the study period, Aqua MODIS recorded SST values ranging from 28°C to 30°C, while the SST values generated by ROMS varied from 26°C to 28°C. The findings indicate that the ROMS model consistently underestimates SST compared to Aqua MODIS, with a persistent discrepancy of 2°C to 3°C. This difference in SST readings may be attributed to several factors, including inaccurate initial conditions, erroneous atmospheric fluxes, boundary conditions, and/or flawed parameterizations within the ROMS model (Baduru et al., 2025). Additionally, it is important to note that Aqua MODIS exclusively measures the ocean's surface temperature, which may not accurately represent the thermal structure of the water column. Consequently, Aqua MODIS SST is often warmer than the bulk temperature of the up-

per mixed layer simulated by ROMS (Costa et al., 2012). Moreover, the presence of clouds and aerosols in the atmosphere can lead to missing data in satellite measurements, further contributing to this observed disparity. Given that the bias is consistent across the datasets, the underestimation of SST by ROMS can be addressed through bias correction techniques to reduce prediction errors (Soriano et al., 2019).

It is observed that both SST datasets exhibit a variable pattern, characterized by peaks occurring in the early part of the month. In mid-November, both datasets reveal a more stable or minor change in SST. As early December approaches, a slight decrease in SST is noted, following a significant peak observed in late November. Throughout mid-December, minor fluctuations accompanied by a downward trend in SST suggest a cooling trend in SSTs, which persists until the end of the month. This indicates that, despite some discrepancies between the datasets, their fluctuating characteristics remain consistent throughout the study period. The abrupt changes in fluctuation patterns may be attributed to seasonal transitions. Both months fall within the Northeast Monsoon (NEM) season, with the full onset of NEM, characterized by heavy rainfall, occurring in late November, which contributes to the observed cooling of SST during this timeframe.

4.2 Linear Modeling plot

The linear modelling plot illustrates a scatter plot comparing SST data obtained from Aqua-MODIS with SST data derived from the ROMS model. In this plot, Aqua MODIS data is represented on the x-axis, while ROMS data is displayed on the y-axis, accompanied by a reference line denoting $y = x$. The accuracy of the modelled data can be assessed by examining how the scatter plot deviates from this 1:1 line. A plot that aligns with the reference line indicates a perfect correlation between the two datasets, whereas any deviation from this line reveals whether the modelled data is lower or higher than the observed data (Sengupta and Jammalamadaka, 2003). In this study, the scatter plot for all six locations is situated below the reference line, suggesting that the modelled SST values are lower and exhibit a positive correlation with the Aqua MODIS SST values (Figure 3). This finding indicates an underestimation of the ROMS SST, which generally follows a trend similar to that of the Aqua MODIS SST data. Such comparable characteristics were also observed in the time series plot.

4.3 Taylor diagram plot

To gain a more comprehensive understanding of the performance of the ROMS SST, Taylor diagrams were constructed using datasets from six distinct locations (Figure 4). The average value across these six locations was also represented as an 'x' on the diagram. In this visualization, the black star denotes the reference point, characterized by a

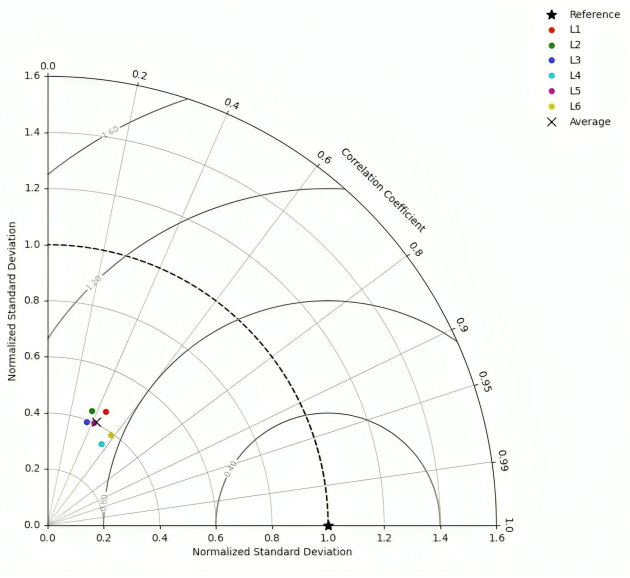

Figure 4. Taylor diagram featuring location points designated as L1, L2, L3, L4, L5, and L6, along with a composite average point representing all locations.

correlation coefficient of 1 and a normalized standard deviation of 1, indicating a perfect alignment with an RMSE of 0. Each of the six locations' ROMS SST values was color-coded, and their positions on the diagram reflect the degree of similarity between the simulated data and the reference datasets. The current analysis reveals that the correlation coefficients for locations L4 and L6 are approximately 0.6, suggesting a relatively strong correlation compared to other locations, where the correlation coefficients fall below 0.6, indicating weak to moderate correlations between ROMS and Aqua-MODIS SST. The normalized standard deviations for all location points are below 1.0, with some even under 0.5, signifying that the variability in ROMS SST is less pronounced compared to the reference data from Aqua-MODIS satellite observations. The black 'x', representing the average of the locations, indicates that the ROMS predictions are generally average when compared to Aqua-MODIS observations, with a moderate correlation value of approximately 0.5, reflecting an almost linear relationship. The reduced variability of ROMS SST relative to satellite observations is evidenced by a moderately low normalized standard deviation of around 0.4. This limited variability suggests that the model captures only about 40% of the variability present in Aqua-MODIS satellite data, likely due to inaccuracies in input conditions or insufficient satellite data. Both the moderate correlation and standard deviation indicate a moderate level of agreement between ROMS and Aqua-MODIS SST data (Taylor, 2001). In summary, the average characteristics of the locations suggest that no specific location stands out as superior to the others. The Taylor diagram indicated that additional enhancements are required to achieve a closer alignment

between the modelled datasets and the reference dataset.

4.4 Error metrics calculation

The inconsistencies between the SST values modelled by the ROMS and those observed by Aqua-MODIS at six distinct locations were also assessed using error metrics, specifically RMSE and MAE (Table 3). The RMSE values ranged from 2.15 to 3.03, with an average of 2.58°C, while the MAE values varied from 2.05 to 2.94, averaging 2.50°C. These metrics indicate that the ROMS model tends to underestimate SST by approximately 2.5°C in comparison to Aqua-MODIS data. The lowest error was recorded at location L5, whereas the highest was observed at L2. The estimated errors across all locations exhibited minimal variation, suggesting that the simulated SST values do not significantly outperform or underperform across the six sites. Furthermore, the RMSE was consistently higher than the MAE at all locations, indicating the presence of some outliers in the ROMS predictions; however, the differences between RMSE and MAE were not substantial enough to suggest that these outliers are particularly significant (Chai and Draxler, 2014). Consequently, it is evident that L5 is the most accurate location, with ROMS-simulated SST values closely aligning with Aqua-MODIS observations, while L2 demonstrates comparatively poorer performance with greater error estimates.

Table 3. RMSE and MAE for locations L1, L2, L3, L4, L5, and L6.

Location	RMSE	MAE
L1	2.66	2.55
L2	3.03	2.94
L3	2.49	2.39
L4	2.43	2.37
L5	2.15	2.05
L6	2.76	2.71
Average	2.58	2.50

4.5 Bias correction

The analysis presented in the preceding section indicates a clear necessity for adjustments to the ROMS-modelled SST dataset in order to align it with the Aqua-MODIS observed SST dataset. Given the consistent biases across the datasets, various bias correction techniques can be employed to rectify the modelled SST. This study examines three specific bias correction methods: the DC, LS, and QM. The objective is to determine which of these methods is most effective for correcting the modelled SST data from ROMS. The evaluation of the corrected datasets was conducted through time-series plots and statistical analyses, including RMSE, MAE, and the correlation coefficient (r).

4.5.1 Time-series plot

A time-series plot illustrating the original ROMS SST, SST from Aqua MODIS, and bias-corrected ROMS SST using the DC, LS, and QM methods was created for the period from November 1 to December 31, 2019, as shown in Figure 5. Notable enhancements in the alignment of ROMS-simulated SST were observed across all three correction techniques, effectively addressing the datasets' underestimation. The results from the DC method indicated an upward shift in the SST modeled by ROMS, primarily achieved by analyzing the discrepancies between Aqua MODIS and ROMS SST data. However, this correction did not significantly alter the original distribution pattern of ROMS SST. Similarly, while the SST corrected by the LS method was closely aligned with Aqua MODIS SST, it failed to preserve the original distribution pattern of the Aqua MODIS data. The LS method involved a linear transformation of the modeled data, estimating the scale factor and additive bias through regression analysis. Although both the DC and QM corrected ROMS SST exhibited similar patterns in the time series distribution, the QM method demonstrated superior performance by effectively capturing most fluctuations in Aqua MODIS SST. Overall, the time series plot indicates that the QM method yielded better results for ROMS SST compared to the other two methods. To further evaluate the most appropriate bias correction method, error metric calculations were also conducted.

4.5.2 Statistical comparison with error metrics

Estimation of error metrics for the bias-corrected ROMS SST at six locations was conducted, with results presented in Table 4. For the original ROMS SST, the RMSE varied between 2.15 and 3.03, yielding an average of 2.58. The highest RMSE was recorded at location L2, while the lowest was at L5. The MAE ranged from 2.05 to 2.94, with an average of 2.50, again showing the highest value at L2 and the lowest at L5. The correlation coefficient for the original ROMS SST spanned from 0.17 to 0.46, averaging 0.30; the lowest value was observed at L3, and the highest at L4. In the case of the DC corrected ROMS SST, the lowest RMSE values were found at locations L4 and L6, while the highest was at L1, resulting in an average RMSE of 0.64. The MAE ranged from 0.40 to 0.55, with an average of 0.48, where the lowest value was at L6 and the highest at L1. The correlation coefficient for the DC-corrected ROMS SST varied from 0.17 (L3) to 0.46 (L4), maintaining an average of 0.30. For the LS corrected ROMS SST, the RMSE ranged from 0.49 at L6 to 0.61 at L3, with an average of 0.56. The MAE in this scenario varied from 0.41 (L6) to 0.55 (L2), averaging 0.48. The correlation coefficient for the LS corrected ROMS SST showed a range from 0.17 (L3) to 0.46 (L4), with an average of 0.30. Regarding the quantile mapping (QM) corrected ROMS SST, the RMSE and MAE values ranged from 0.58 to 0.74 and 0.45 to 0.58, respectively. The lowest RMSE was recorded at L6, while L5 exhibited the lowest MAE; conversely, L1 had the highest values for both RMSE and MAE. The average RMSE and MAE were 0.67 and 0.51, respectively. The correlation coefficient for the QM corrected ROMS SST showed a range from 0.26 (L1) to

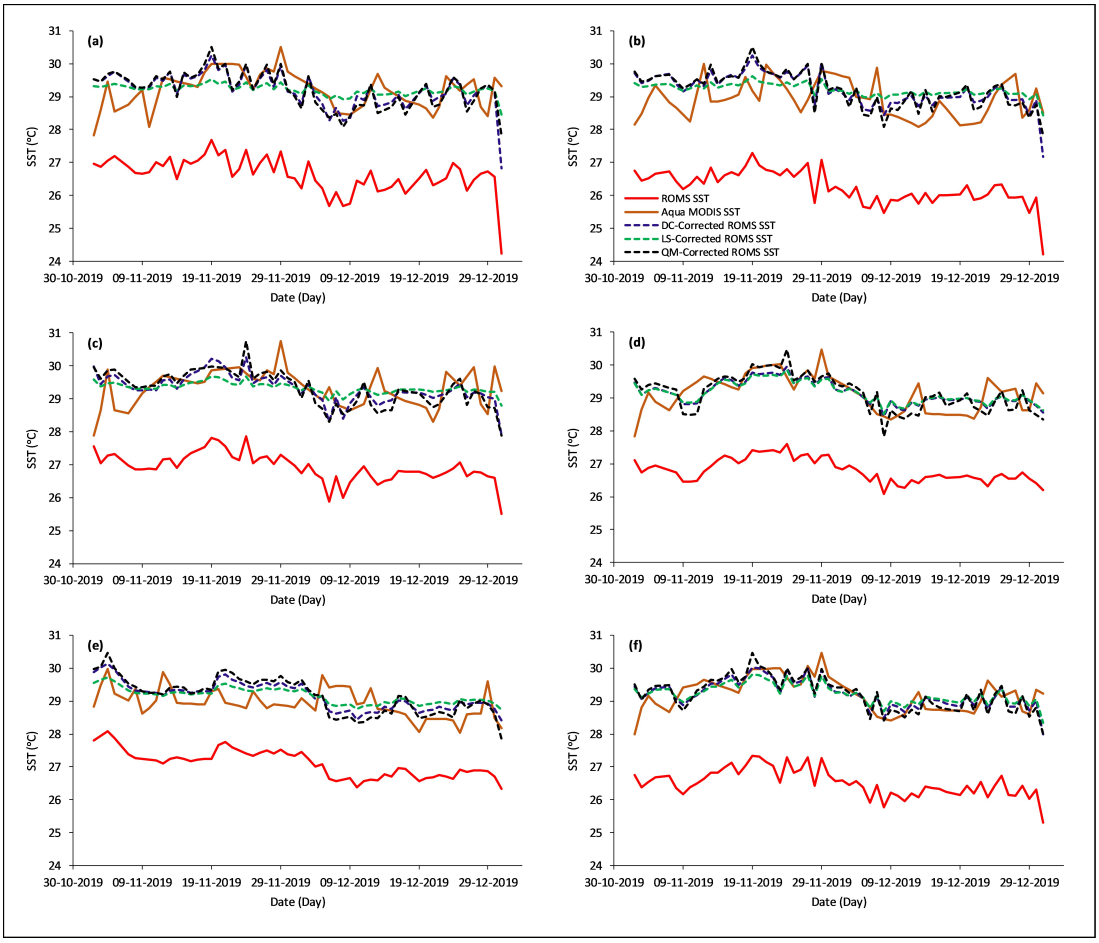

Figure 5. Time series plot comparing the corrected and original ROMS SST data with Aqua-MODIS SST measurements for the period from November to December 2019 at the following locations: (a) L1, (b) L2, (c) L3, (d) L4, (e) L5, and (f) L6.

Table 4. RMSE, MAE and correlation coefficient (r) for the original, DC, LS, and QM-corrected ROMS SST at the specified locations L1, L2, L3, L4, L5, and L6, along with their averages.

		L1	L2	L3	L4	L5	L6	AVG
Original	RMSE	2.65	3.03	2.49	2.43	2.15	2.76	2.58
	MAE	2.55	2.94	2.39	2.37	2.05	2.71	2.50
	r	0.22	0.24	0.17	0.46	0.27	0.45	0.30
DC	RMSE	0.75	0.72	0.70	0.52	0.62	0.52	0.64
	MAE	0.55	0.53	0.54	0.41	0.46	0.40	0.48
	r	0.22	0.24	0.17	0.46	0.27	0.45	0.30
LS	RMSE	0.59	0.59	0.61	0.52	0.56	0.49	0.56
	MAE	0.50	0.55	0.51	0.42	0.47	0.41	0.48
	r	0.22	0.24	0.17	0.46	0.27	0.45	0.30
QM	RMSE	0.74	0.73	0.66	0.66	0.68	0.58	0.67
	MAE	0.58	0.54	0.54	0.51	0.45	0.46	0.51
	r	0.26	0.28	0.27	0.36	0.34	0.44	0.33

0.44 (L6), with an average of 0.33.

The bias-corrected SST demonstrates a notable enhancement when compared to the original ROMS SST. The SST adjusted using the LS method exhibits improved average values for both RMSE and MAE, while the correlation coefficient remains unchanged from that of the original SST. Similarly, the correction applied through the DC method also yields better RMSE and MAE results, yet the correlation coefficient remains consistent with the original values. In contrast, the QM method shows an improvement in the correlation coefficient compared to the other two correction methods. Overall, the bias correction of ROMS SST

utilizing the QM method results in superior performance relative to the other two approaches.

5. Conclusion

Given the inherent challenges of predicting SST in a coastal setting marked by significant dynamism and complexity, this research successfully utilized and thoroughly investigated the efficacy of the ROMS, a high-resolution modeling framework, in forecasting SST in the northern coastal area of Penang Island, Malaysia. The initial phase of the study involved the establishment of a robust methodology, which included the generation of the model through the specification of input grid domains, atmospheric forcing, boundary conditions, and initialization processes. The analysis reveals, through the Time series plot, Linear Modelling plot, and Taylor diagram, that the ROMS model consistently underestimates SST across the six locations examined in this study. A discrepancy of 2 to 3°C was observed between the SST values generated by the ROMS model and those obtained from Aqua MODIS. The time series plot indicates that the SST predictions from the ROMS model were consistently 2 to 3°C lower than the satellite data from Aqua MODIS at all six sites. The Taylor diagram illustrates that while the model demonstrates improved accuracy in certain locations (specifically L4 and L6), it only achieves a 40% similarity with Aqua MODIS data. Furthermore, the model's performance was assessed using error estimation techniques, including RMSE and MAE, yielding average values of 2.58°C and 2.50°C, respectively, which further highlight the existing discrepancies.

The current study evaluated three distinct bias correction techniques: DC, LS, and QM, aimed at enhancing the accuracy of SST simulations derived from the ROMS model. A comparative analysis utilizing time series plots of SST across six locations demonstrated that these bias correction methods effectively mitigate model bias. The bias-corrected SST exhibited average error estimation values ranging from 0.45 to 0.70 for both RMSE and MAE. Notably, while the DC and LS methods did not enhance the correlation between the ROMS outputs and observed data, LS was effective in minimizing mean errors.

Conversely, the QM method achieved a balanced correction, leading to improved correlation values by addressing both mean bias and variability, thereby making it a suitable approach for refining SST predictions from the ROMS model. Overall, the findings indicate that the ROMS model is a valuable tool for simulating SST, despite its tendency to underestimate SST; it successfully captures the variability within the study area. To further enhance prediction accuracy, the incorporation of alternative atmospheric forcing files is recommended. Additionally, the study utilized the HYCOM model for boundary and initialization files, suggesting that exploring other ocean models could also improve ROMS predictions. Furthermore, to maintain trends in the predicted data, alternative techniques such as quantile delta mapping (QDM) or detrended quantile mapping (DQM) could be integrated.

Acknowledgements

All authors would like to express sincere gratitude to the Universiti Sains Malaysia (USM) for the support during the preparation of the manuscript. Authors are also thankful to Chua Seong Jinq and Satpal Singh for their support during the data analysis. Authors extend their sincere thanks to the anonymous reviewers and Editor-in-Chief Prof. Jacek Piskozub, for their critical review, constructive comments and suggestions, which improved the quality of the manuscript.

Authors' contributions

NKMV, CA, YY contributed to the study conception and design. Material preparation, data collection and analysis were performed by CA, NKMV, ABA, EJJ and YY. The first draft of the manuscript was written by NKMV. YY commented on previous versions of the manuscript. All authors read and approved the final manuscript.

Conflict of interest

None declared.

References

Acharya, N., Chattopadhyay, S., Mohanty, U.C., Dash, S.K., Sahoo, L.N., 2013. *On the bias correction of general circulation model output for Indian summer monsoon*. Meteorol. Appl. 20, 349–356. https://doi.org/10.1002/met.1294

Alizadeh, O., 2022. *Advances and challenges in climate modeling*. Climatic Change 170, 18. https://doi.org/10.1007/s10584-021-03298-4

Baduru, B., Paul, B., Athul, C.R., Paul, A., Francis, P.A., 2025. *Improving Indian Ocean analysis using ROMS with sea level anomaly assimilation*. J. Earth Sys. Sci.134 (2), 1–19. https://doi.org/10.1007/s12040-025-02587-1

Barton, I.J., 1995. *Satellite-derived sea surface temperatures: Current status*. J. Geophys. Res.-Oceans 100 (C5), 8777–8790.

Beyer, R., Krapp, M., Manica, A., 2020. *An empirical evaluation of bias correction methods for palaeoclimate simulations*. Clim. Past 16 (4), 1493–1508. https://doi.org/10.5194/cp-16-1493-2020

Casey, K.S., Cornillon, P., 1999. *A comparison of satellite and in situ–based sea surface temperature climatologies*. J. Climate 12 (6), 1848–1863.

Chai, T., Draxler, R.R., 2014. *Root mean square error (RMSE) or mean absolute error (MAE)? – Arguments against avoiding RMSE in the literature*. Geosci. Model Dev. 7

(3), 1247–1250.
https://doi.org/10.5194/gmd-7-1247-2014

Costa, P., Gómez, B., Venâncio, A., Pérez, E., Pérez-Muñuzuri, V., 2012. *Using the Regional Ocean Modelling System (ROMS) to improve the sea surface temperature predictions of the MERCATOR Ocean System*. Sci. Mar. 76 (S1), 165–175.
https://doi.org/10.3989/scimar.03614.19E

Cunnane, C., 1989. *Statistical distribution for flood frequency analysis*. WMO Operational Hydrology, Rep. No. 33, WMO-No. 718, Geneva, Switzerland.

Dhawan, P., Dalla Torre, D., Niazkar, M., Kaffas, K., Larcher, M., Righetti, M., Menapace, A., 2024. *A comprehensive comparison of bias correction methods in climate model simulations: Application on ERA5-Land across different temporal resolutions*. Heliyon 10 (23).
https://doi.org/10.1016/j.heliyon.2024.e40352

Dubovik, O., Schuster, G.L., Xu, F., Hu, Y., Bösch, H., Landgraf, J., Li, Z., 2021. *Grand Challenges in Satellite Remote Sensing*. Front. Remote Sens. 2.
https://doi.org/10.3389/frsen.2021.619818

Embury, O., Merchant, C.J., Good, S.A., Rayner, N.A., Høyer, J.L., Atkinson, C., Block, T., Alerskans, E., Pearson K.J., Worsfold, M., McCarroll, N., Donlon, C., 2024. *Satellite-based time-series of sea-surface temperature since 1980 for climate applications*. Sci. Data 11 (1), 326.
https://doi.org/10.1038/s41597-024-03147-w

Guan, X., Huang, H., Ke, X., Cheng, X., Zhang, H., Chen, A., Qiu, G., Wu, H., Wei, C., 2025. *Monitoring, modeling, and forecasting long-term changes in coastal seawater quality due to climate change*. Nat. Commun. 16 (1), 2616.
https://doi.org/10.1038/s41467-025-57913-4

Guild, R., Wang, X., Quijón, P. A. 2025. *Climate change impacts on coastal ecosystems*. Environ. Res.: Climate, 3 (4), 042006.

Haghbin, M., Sharafati, A., Motta, D., Al-Ansari, N., Noghani, M.H.M., 2021. *Applications of soft computing models for predicting sea surface temperature: a comprehensive review and assessment*. Prog. Earth Planet. Sci. 8, 1–19.
https://doi.org/10.1186/s40645-020-00400-9

Han, S., Wang, Z., 2022. *Simulation of seasonal variation characteristics of offshore water temperature based on ROMS model*. Proc. 2022 Global Reliability and Prognostics and Health Management (PHM-Yantai). IEEE, Yantai, China, 1–6.

Hewitt, J.E., Ellis, J.I., Thrush, S.F. 2016. *Multiple stressors, nonlinear effects and the implications of climate change impacts on marine coastal ecosystems*. Glob. Change Bio. 22 (8), 2665–2675.
https://doi.org/10.1111/gcb.13176

Hobday, A.J., Alexander, L.V., Perkins, S.E., Smale, D.A., Straub, S.C., Oliver, E.C., Benthuysen, J.A., Burrows, M.T., Donat, M.G., Feng, M., Holbrook, N.J., Moore, P.J., Scannell, H.A., Gupta, A.S., Wernberg, T., 2016. *A hierarchical approach to defining marine heatwaves*. Prog. Oceanog. 141, 227–238.
https://doi.org/10.1016/j.pocean.2015.12.014

Huang, B., Liu, C., Banzon, V., Freeman, E., Graham, G., Hankins, B., Smith, T., Zhang, H.M., 2021. *Improvements of the Daily Optimum Interpolation Sea Surface Temperature (DOISST) Version 2.1*. J. Climate 34 (8), 2923–2939.
https://doi.org/10.2307/27076773

Jose, D.M., Dwarakish, G.S., 2022. *Bias Correction and Trend Analysis of Temperature Data by a High-Resolution CMIP6 Model over a Tropical River Basin*. Asia-Pac. J. Atmos. Sci. 58 (1), 97–115.
https://doi.org/10.1007/s13143-021-00240-7

Kaewmesri, P., 2019. *Simulation sea surface temperature over Gulf of Thailand by using ROMS model*. Int. J. GEOMATE 17 (60), 56–61.
https://doi.org/10.21660/2019.60.4709

Kartal, S., 2023. *Assessment of the spatiotemporal prediction capabilities of machine learning algorithms on Sea Surface Temperature data: A comprehensive study*. Eng. Appl. Artif. Intel. 118.
https://doi.org/10.1016/j.engappai.2022.105675

Kilpatrick, K.A., Podestá, G.P., Evans, R., 2001. *Overview of the NOAA/NASA advanced very high resolution radiometer Pathfinder algorithm for sea surface temperature and associated matchup database*. J. Geophys. Res.-Oceans 106 (C5), 9179–9197.

Kushwaha, P., Pandey, V.K., Das, B.K., Singh, Y., Srivastav, S., 2024. *Exploring temporal and spatial SST patterns and their impact in the Arabian Sea: Insights from the regional ocean modeling system*. Cont. Shelf. Res. 275.
https://doi.org/10.1016/j.csr.2024.105224

Lemos, G., Menendez, M., Semedo, A., Camus, P., Hemer, M., Dobrynin, M., Miranda, P.M., 2020. *On the need of bias correction methods for wave climate projections*. Global Planet. Change 186.
https://doi.org/10.1016/j.gloplacha.2019.103109

Li, Z.L., Wu, H., Duan, S.B., Zhao, W., Ren, H., Liu, X., Leng, P., Tang, R., Ye, X., Zhu, J., Sun, Y., Si, M., Liu, M., Li, J., Zhang, X., Shang, G., Tang, B., Yan, G., Zhou, C., 2023. *Satellite Remote Sensing of Global Land Surface Temperature: Definition, Methods, Products, and Applications*. Rev. Geophys. 61.

Mann, K.H., Lazier, J.R., 2005. *Dynamics of marine ecosystems: biological-physical interactions in the oceans*. John Wiley & Sons.

McPhaden, M.J., Zebiak, S.E., Glantz, M.H., 2006. *ENSO as an Integrating Concept in Earth Science*. Science 314 (5806), 1740–1745.

Mendez, M., Maathuis, B., Hein-Griggs, D., Alvarado-Gamboa, L.F., 2020. *Performance evaluation of bias correction methods for climate change monthly precipitation projections over Costa Rica*. Water 12 (2), 482.

https://doi.org/10.3390/w12020482

Merchant, C.J., Embury, O., Bulgin, C.E., Block, T., Corlett, G.K., Fiedler, E., Good, S.A., Mittaz, J., Rayner, N.A., Berry, D., Eastwood, S., Taylor, M., Tsushima, Y., Waterfall, A., Wilson, R., Donlon, C., 2019. *Satellite-based time-series of sea-surface temperature since 1981 for climate applications*. Sci. Data 6 (1), 223. https://doi.org/10.1038/s41597-019-0236-x

O'Carroll, A.G., Armstrong, E.M., Beggs, H.M., Bouali, M., Casey, K.S., Corlett, G.K., Dash, P.,Donlon, C.J., Gentemann, C.L., Høyer, J.L., Ignatov, A., Kabobah, K., Kachi, M., Kurihara, Y., Karagali, I., Maturi, E., Merchant C.J., Marullo, S., Minnett, P.J., Pennybacker, M., Ramakrishnan, B., Ramakrishnan, R., Santoleri, R., Sunder, S., Picart, S.S., Vázquez-Cuervo, J., Wimmer, W., 2019. *Observational needs of sea surface temperature*. Front. Mar. Sci. 6, 420.

Ottersen, G., Stenseth, N.C., Hurrell, J.W., 2004. *Climatic fluctuations and marine systems: A general introduction to the ecological effects*. [In:] *Marine Ecosystem and Climate Variation*, Stenseth, N.Chr., Geir, O. (Eds.), 3–14.

Piccolo, M.C., 2021. *Effects of rainfall extreme events on coastal marine ecosystems*. [In:] *Precipitation*, Rodrigo-Comino, J. (Ed.), Elsevier, 261–285.

Ringard, J., Seyler, F., Linguet, L., 2017. *A quantile mapping bias correction method based on hydroclimatic classification of the Guiana shield*. Sensors. 17 (6), 1413. https://doi.org/10.3390/s17061413

Satar, M.N., Marshal, W., Akhir, M.F., 2024. *The Effects of Climate Change on Ocean Upwelling and Productivity in Regional Seas*. [In:] *Coastal Sustainability*, Maccarrone, V., Fadzil Akhir, M. (Eds.), Coastal Research Library. 21–49.

Sengupta, D., Jammalamadaka, S.R., 2003. *Linear models: an integrated approach*. World Sci., 644 pp.

Shevchenko, G.V., Tshay, Z.R., Lozhkin, D.M., 2024. *Spatiotemporal Variability of Bering Sea Surface Temperature from Satellite-Based ERA5 Reanalysis Data*. Izv., Atmos. Ocean. Phys. 60 (9), 1075–1085. https://doi.org/10.1134/S0001433824701032

Soriano, E., Mediero, L., Garijo, C., 2019. *Selection of bias correction methods to assess the impact of climate change on flood frequency curves*. Water 11 (11). https://doi.org/10.3390/w11112266

Taylor, K.E., 2001. *Summarizing multiple aspects of model performance in a single diagram*. J. Geophys. Res.-Atmos. 106 (D7),7183–7192.

Tiwari, P., Dimri, A.P., Shenoi, S.C., Francis, P.A., Jithin, A.K., 2021. *Impact of Surface forcing on simulating Sea Surface Temperature in the Indian Ocean – A study using Regional Ocean Modeling System (ROMS)*. Dynam. Atmos. Oceans 95. https://doi.org/10.1016/j.dynatmoce.2021.101243

Vanem, E., Zhu, T., Babanin, A., 2022. *Statistical modelling of the ocean environment – A review of recent developments in theory and applications*. Mar. Struct. 86. https://doi.org/10.1016/j.marstruc.2022.103297

Wang, B., Hua, L., Mei, H., Wu, X., Kang, Y., Zhao, N., 2024. *Impact of Climate Change on the Dynamic Processes of Marine Environment and Feedback Mechanisms: An Overview*. Arch. Comput. Method E. 31 (6), 3377–3408.

Whitney, F.A., Crawford, W.R., Harrison, P.J., 2005. *Physical processes that enhance nutrient transport and primary productivity in the coastal and open ocean of the subarctic NE Pacific*. Deep Sea Research Pt. II, 52 (5–6), 681–706.

Williams, R.G., Follows, M.J., 2003. *Physical Transport of Nutrients and the Maintenance of Biological Production*. [In:] *Ocean Biogeochemistry*. Springer, Berlin, Heidelberg, 19–51.

Zrira, N., Kamal-Idrissi, A., Farssi, R., Khan, H.A., 2024. *Time series prediction of sea surface temperature based on BiLSTM model with attention mechanism*. J. Sea. Res. 198. https://doi.org/10.1016/j.seares.2024.102472